This is the accepted manuscript of the article, which has been published in Journal of the american chemical society. 2019, 141(41), 16303-16311 https://doi.org/10.1021/jacs.9b06036

Competition for membrane receptors: norovirus detachment via lectin attachment

Nagma Parveen[1,], Gustaf E. Rydell[2], Göran Larson[3], Vesa P. Hytönen[4], Vladimir P. Zhdanov[1,5], Fredrik Höök[1*], Stephan Block[1,†*]*

[1]Department of Physics, Chalmers University of Technology, Gothenburg, Sweden

[2]Department of Infectious Diseases, Sahlgrenska Academy, University of Gothenburg, Gothenburg, Sweden

[3]Department of Laboratory Medicine, Sahlgrenska Academy, University of Gothenburg, Gothenburg, Sweden

[4]Faculty of Medicine and Health Technology and BioMediTech, Tampere University, Tampere, Finland and Fimlab Laboratories, Tampere, Finland

[5]Boreskov Institute of Catalysis, Russian Academy of Sciences, Novosibirsk, Russia

*Laboratory for Photochemistry and Spectroscopy, Department of Chemistry, KU Leuven, Leuven, Belgium

[†]Department of Chemistry and Biochemistry, Free University of Berlin, Berlin, Germany

Keywords: norovirus–like particle, histo–blood group antigens, glycosphingolipid, lectin, supported lipid bilayer, competitive inhibition, release kinetics, multivalent interaction

Abstract

Virus internalization into the host cells occurs via multivalent interactions, in which a single virus binds to multiple receptors in parallel. Because of analytical and experimental limitations this complex type of interaction is still poorly understood and quantified. Herein, the multivalent interaction of norovirus-like particles (noroVLPs) with H or B type 1 glycosphingolipids (GSLs), embedded in a supported phospholipid bilayer, is investigated by following the competition between noroVLPs and a lectin (from *Ralstonia solanacearum*) upon binding to these GSLs. Changes in noroVLP and lectin coverage, caused by competition, were monitored for both GSLs and at different GSL concentrations using quartz crystal microbalance with dissipation monitoring. The study yields information about the minimum GSL concentration needed for i) noroVLPs to achieve firm attachment to the bilayer prior to competition, and to ii) remain firmly attached to the bilayer during competition. We show that these two concentrations are almost identical for the H type 1–noroVLP interaction, but differ for B type 1, indicating an accumulation of B type 1 GSLs in the noroVLP–bilayer interaction area. Furthermore, the GSL concentration required for firm attachment is significantly larger for H type 1 than for B type 1, indicating a higher affinity of noroVLP towards B type 1. This finding is supported by extracting the energy of single noroVLP–H type 1 and noroVLP–B type 1 bonds from the competition kinetics, which were estimated to be 5 and 6 kcal/mol, respectively. This demonstrates the potential of utilizing competitive binding kinetics to analyse multivalent interactions, which has remained difficult to quantify using conventional approaches.

Introduction

The interaction of biological nanoparticles, such as viruses, extracellular vesicles and drug delivery vehicles, with the plasma membrane typically involves multiple ligands and membrane receptors (*i.e.*, attachment factors) either of the same or different types. The ligands belonging to the nanoparticles can be either fixed or mobile, whereas receptors are typically mobile within the membranes of host cells.[1-3] Although the energy of a single ligand-receptor bond is relatively weak (*e.g.*, 1–5 kcal/mol or K_d of 0.1–5 mM for polyoma- and human noroviruses binding to glycosphingolipids)[4-7], formation of multiple bonds results in a strong enough attachment of the virus particles to cell membranes.[8-9] Multivalent interactions of this type are most commonly investigated by measuring interaction kinetics at varying receptor coverage in the membrane,[6, 10-11] or by inhibiting the interaction by addition of compounds designed to interact with the ligands on suspended nanoparticles.[8, 12] In the particular case of virus binding, it is also common to interfere with the ligand-receptor interaction by addition of compounds designed to bind with appreciable affinity to the cell-membrane receptors.[13-14] This approach has turned out especially interesting in the context of antiviral drugs[15-17] as in the case of HIV-1, where it has even reached clinical applications.[18]

However, in contrast to classical surface chemistry, where the formalism describing the interplay of adsorption and desorption under competitive conditions is well established[19-21], competitive binding of different biological nanoparticles to cell membranes is less understood. In conventional surface chemistry, the adsorption sites generally reside on a firm support and the state of an adsorbed atom or molecule is primarily influenced via lateral interactions with neighbouring adsorbed atoms or molecules, while in the case of multivalent interactions on cellular membranes, the receptor-mediated binding can in addition be weakened by competing entities that reduce the concentration of mobile receptors available for binding. Such competitive binding can be utilized to probe the binding affinity of viruses towards different receptor-containing cell membranes.[6, 15-16] Moreover, the competitive binding may provide a better insight to the complicated pathways of cellular internalization of viruses, aiding the development of antiviral drugs.

One of the key challenges in the context of measuring competitive binding between different types of biomolecules is that they need to be individually identified using a unique fingerprint. Most methods suitable for studying biomolecular interactions probe ligand-receptor interactions using soluble isolated biomolecules [such as nuclear magnetic resonance (NMR) spectroscopy, isothermal titration calorimetry, etc.]. In contrast, surface-based methods such as for example surface plasmon resonance or surface quartz crystal microbalance with dissipation (QCM-D) provide platforms to reconstitute receptors or ligands in lipid membranes, attaining native-like environment for binding kinetic studies. QCM-D offers the additional opportunity to distinguish different ligand variants given that they contribute differently to measured changes in frequency, Δf, and energy dissipation, ΔD, upon binding to the QCM sensor surface. Aided by this capacity, we recently explored competitive binding interactions between cholera toxin and virus-like particles (VLPs) made from SV40 virus to their common GM1 receptor, and demonstrated how QCM-D monitoring could be used to quantify the kinetics of the interaction.[6] In the present work, we put emphasis on VLPs made from the major viral protein (VP1) of human norovirus, which is particularly interesting in this context since it has been hypothesized that upon infection, noroviruses increase their chance of host infection *via* cellular attachment and subsequent internalization by binding to closely resembling yet different attachment factors.[22-23] More specifically, we made use of competitive binding between norovirus-like particles (noroVLPs; ~40 nm in diameter) and a lectin (*i.e.*, a carbohydrate-binding protein; ~4.5 nm in diameter) extracted from the bacterium *Ralstonia solanacearum*, which are both capable of binding specifically to the glycosphingolipids (GSLs) H type 1 and B type 1.[4, 24-26] Using QCM-D, we explored how addition of the lectin triggers release of noroVLPs from GSL-containing supported lipid bilayers (SLBs) and how this competition between lectins and noroVLPs for the same GSL can be employed to determine the affinity of the GSL-noroVLPs interaction. We also demonstrated that a single competitive binding experiments is sufficient to accurately quantify the minimum GSL concentration required for noroVLPs to remain firmly attached to the SLB and that variations in multivalency for GSLs with different affinity can in this way be readily identified.

Materials, methods, and sample preparation

Materials. Histo-blood group antigens (HBGAs) in form of the GSLs H type 1 (M = 1.28 kDa) and B type 1 (M = 1.45 kDa) were isolated from total non-acid GSL fractions purified from human meconia, pooled according to ABO blood group, and characterized by mass spectrometry and 1H-NMR spectroscopy.[27] Partially hexahistidine-tagged noroVLPs (with diameter 40±10 nm according to electron microscopy images) of GII.4 strain were expressed and characterized as detailed in Koho *et al*.[28] VP1 is the major viral protein of the noroVLP and binds to H type 1 or B type 1 HBGAs. While most studies have shown that each VP1 proteins contains at least one binding site for HBGAs[29], a recent report provided evidence that VP1 can bind to two HBGAs in parallel, thereby suggesting the presence of two HBGA binding sites per VP1.[30] In total, 180 copies of the VP1 protein assemble into a noroVLP, leading to a density of 0.035 or 0.071 HBGA binding sites per nm^2 on the capsid surface (calculating with 1 and 2 binding sites per VP1, respectively). 1-palmitoyl-2-oleoyl-sn-glycero-3-phosphocholine (POPC) and lectin from bacterium *Ralstonia solanacearum* (RSL) were purchased from Avanti Polar Lipids (USA) and Elicityl OligoTech (Crolles, France), respectively. The RSL lectin (having a beta-barrel structure with diameter of 4.5 nm)[24] is a hexavalent fucose-binding lectin with K_d (monovalent dissociation constant, affinity) of 1.23 ± 0.06 μM towards L-fucose monosaccharide.[24] All the materials were diluted in a degassed phosphate buffer to achieve desired concentrations. The phosphate buffer contained 50 mM Na_2HPO_4, 100 mM NaCl, pH 7.4.

Quartz crystal microbalance with dissipation. In QCM-D measurements, a quartz crystal with high quality factor (typically > 10^6) is excited *via* the piezoelectric effect to vibrate mechanically at its resonance frequency and accompanied overtones. This shear vibration is induced and tracked by an electronic feedback loop, allowing for extracting information about the frequency (f) and dissipative losses (D) for each probed resonance peak. These resonance properties (f and D) change upon adsorption of material onto the QCM-D crystal. The resonance frequencies, for example, generally decrease upon mass increase on the QCM-D crystal, allowing for probing time-dependent adsorption processes with a sensitivity down to the ng/cm^2 scale. Furthermore, the dissipation D is

the energy damping per oscillation cycle of the crystal and indicates how much vibration energy is dissipated during the oscillation, *e.g.*, due to adsorption of a soft film or due to hydrodynamic interaction of particles adsorbed onto the QCM-D crystal. For example, thin and relatively rigid films like SLBs or small proteins have a fairly low additional contribution to the dissipation, while large nanoparticles, such as VLPs, contribute a larger increase in the dissipation as they possess a relatively large hydrodynamic cross-section, inducing a notable viscous friction of the VLPs with the bulk solution during the vibration of the QCM-D crystal; or phrased in other words, the hydrodynamic interaction of flat layers or nm-sized proteins with the bulk is much smaller than that of VLPs, with the consequence that the latter dissipate, due to frictional losses, much more energy during an oscillation cycle, leading to higher dissipation values in QCM-D experiments. In typical QCM-D experiments, shifts in the frequency and dissipation upon molecular adsorption/binding are measured in a time-dependent manner.

Formulation of phospholipid vesicles. POPC (in chloroform) and either of the HBGA GSLs (in 1:1 chloroform:methanol, v/v) were pipetted into a round bottom flask. The lipid mixture was first dried under a gentle N_2 stream and then dried in vacuum (2 hrs) to obtain a thin lipid film. This dried film was hydrated in the phosphate buffer with help of a vortex. Lipid vesicles were prepared by extruding (13 times) this hydrated lipid suspension with polycarbonate filter (Whatman, UK) of 30 nm pore size. Four vesicle compositions were made by mixing desired weight ratio of POPC and GSLs: (*i*) POPC, (*ii*) POPC+3.5 mol% B type 1, (*iii*) POPC+3.9 mol% H type 1, and (*iv*) POPC+6.3 mol% H type 1. The size (diameter) distribution of the extruded vesicles, determined with a Nanoparticle Tracking Analysis (NTA; Malvern, UK) device, exhibits one peak at about 100 nm with a full width at half maxima (FWHM) of 40 nm.

Supported lipid bilayer formation. SLBs were formed by spreading phospholipid vesicles on a silica-coated QCM-D crystal (QSense E4 instrument; QSense, Göteborg, Sweden).[31] The total GSL concentration, *i.e.*, H or B type 1 content in the bilayer was regulated by using a vesicle solution, which was created by mixing pure POPC vesicles with POPC vesicles containing either 3.9 mol% H

type 1 or 3.5 mol% B type 1, respectively, until the desired mol% of GSL to the total POPC lipids has been reached. The only exception to this approach were SLBs containing 6.3 mol% H type 1, which were created using vesicles composed of 6.3 mol% H type 1 and 93.7 mol% POPC lipids. Further details are described in the Supporting information.

Results. High quality SLB formation was verified from a non-monotonic change in QCM-D response with a final frequency shift (Δf) of about −28±3 Hz and dissipation shift (ΔD) of $(0.2\pm0.15)\times10^{-6}$ upon addition of GSL-containing lipid vesicles (Figure S1 in the Supporting Information).[31] Subsequent injection of a noroVLP suspension (Figure 1) resulted in monotonic decrease in Δf (mass uptake) and increase in ΔD (damping), with diminishing rate of binding and saturated responses as the GSL content of the SLB was decreased, while there was no detectable binding to a SLB made of POPC lipids only (data not shown). This confirms that the noroVLP binding was specific to the presence of H or B type 1 in the SLB. The overall attachment appeared to be irreversible (upon washing with buffer) on SLBs with GSL concentrations exceeding 3.9 mol% H type 1 or 0.7mol% B type 1. This is an indication of multivalent binding of the virus at high GSL density resulting in a firm attachment of the virus on SLB. This conclusion is further supported by the non-linear transition of the initial binding rate ($d\Delta f/dt$) of the noroVLP, which at a constant noroVLP concentration showed an inflection point at around 3 mol% H type 1 and 0.5 mol% B type 1, respectively, and a saturation behavior of the binding rate at larger GSL concentrations (Figure 1d). This transition indicates that the noroVLP binding is reaction-limited below 3 mol% H type 1 and 0.5 mol% B type 1, respectively. Above these concentrations, the diffusion of noroVLPs to the SLB controls the virus binding kinetics. This binding behavior is in agreement with previous studies that showed a similar transition in the binding rate at around 3 mol% H type 1 for the GII.4 Dijon strain of norovirus-like particles, which closely resembles the noroVLP used in this work.[10]

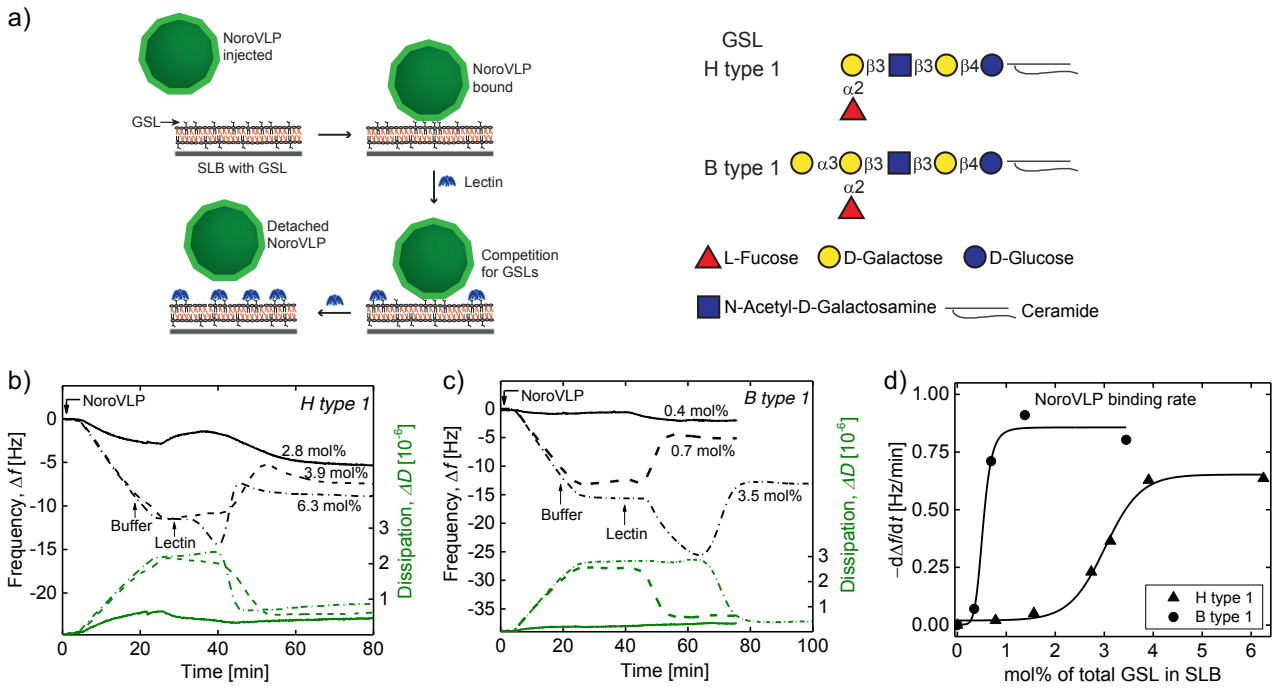

Figure 1. Binding of noroVLPs to a supported lipid bilayer. (a) Left: Schematics of the competitive binding experiments. Right: Chemical composition of H and B type 1 GSLs. The ceramide tail of the GSLs has a heterogeneous composition but it is similar for H and B type 1 as they are extracted from the same natural source. QCM-D time-traces (seventh overtone) upon noroVLP and subsequent lectin binding to SLBs with total (b) H type 1 concentration ranging from 2.8 to 6.3 mol% and (c) B type 1 concentration ranging from 0.4 to 3.5 mol% (as indicated in the plots). The black and green lines correspond to the frequency and dissipation shift, respectively. The arrows indicate the starting moments of solution exchange (the time to reach the measurement chamber was ~4 min at the flow speed used). The binding curves were measured upon subsequent injections of 0.25 nM noroVLP, pure buffer, and lectin at a flow rate of 25 μl/min. 8 nM lectin was used in case of 3.9 mol% H type 1, while 16 and 160 nM lectin was used for all other H and B type 1 contents, respectively. The time axis has been set to zero at the moment of noroVLP injection. SLB formation prior to the noroVLP binding is shown in Figure S1 in the Supporting Information. (d) Initial binding rates were determined from the binding curves shown in Figure S1 based on a linear fit of the phase of linear decrease of Δf. This yields noroVLP binding rates in terms of the rate of the resonance frequency shift, $d\Delta f/dt$, versus the total GSL concentration in the SLB.[32]

Subsequent injection of a competitive ligand, here a fucose-binding lectin isolated from bacterium *Ralstonia solanacearum*, to noroVLP-engaged SLBs causes an overall decrease in ΔD (damping), which is indicative for a release of the SLB-bound noroVLPs (Figure 1b and c).[6] Interestingly, the kinetics of the process varies with the total GSL concentration within the SLB. For example, upon lectin addition to a noroVLP-covered SLB, we observed an initial mass loss (increase in Δf) followed by a mass uptake (decrease in Δf) at < 3.9 mol% H type 1, whereas the kinetics is somewhat more complex at 3.9 mol% and above (Figure 1b and S2a). In the case of B type 1, the VLP release kinetics appear to be very similar, but the transitions are shifted towards lower concentrations of B type 1 in the SLB (Figure 1c and S2b). As discussed further below, to obtain the virus release kinetics within a similar timescale a ten times higher concentration of lectin was used in the case of B type 1 compared to the case of H type 1.

Upon inspection of the frequency traces recorded at high GSL concentrations (3.5 mol% B type 1 and 6.3 mol% H type 1, respectively), it becomes clear that before lectin binding starts to induce noroVLP release, there is a mass uptake (drop in Δf) without any substantial change in ΔD (see dash-dotted lines in Fig. 1b, c and Fig. 2a, c). Supported by the fact that lectin binding to GSL-containing SLBs does not induce appraisable changes in damping (see Figure S3), this mass uptake indicates binding of lectins to the SLB that is not associated with release of noroVLPs, *i.e.*, lectins binding to free GSLs in the bilayer (not being engaged in noroVLP attachment). As described previously,[6] an insignificant change in ΔD upon competitive binding with different ΔD and Δf signatures, makes it possible to deconvolute the measured frequency trace into two separate frequency traces representing the binding kinetics of noroVLPs and lectin, respectively (Figure 2). Further results of this deconvolution procedure are shown in Figures S5 and S7, demonstrating that lectin addition eventually leads to complete release of the SLB-bound noroVLPs irrespective of the H type 1 or B type 1 concentration within the SLB.

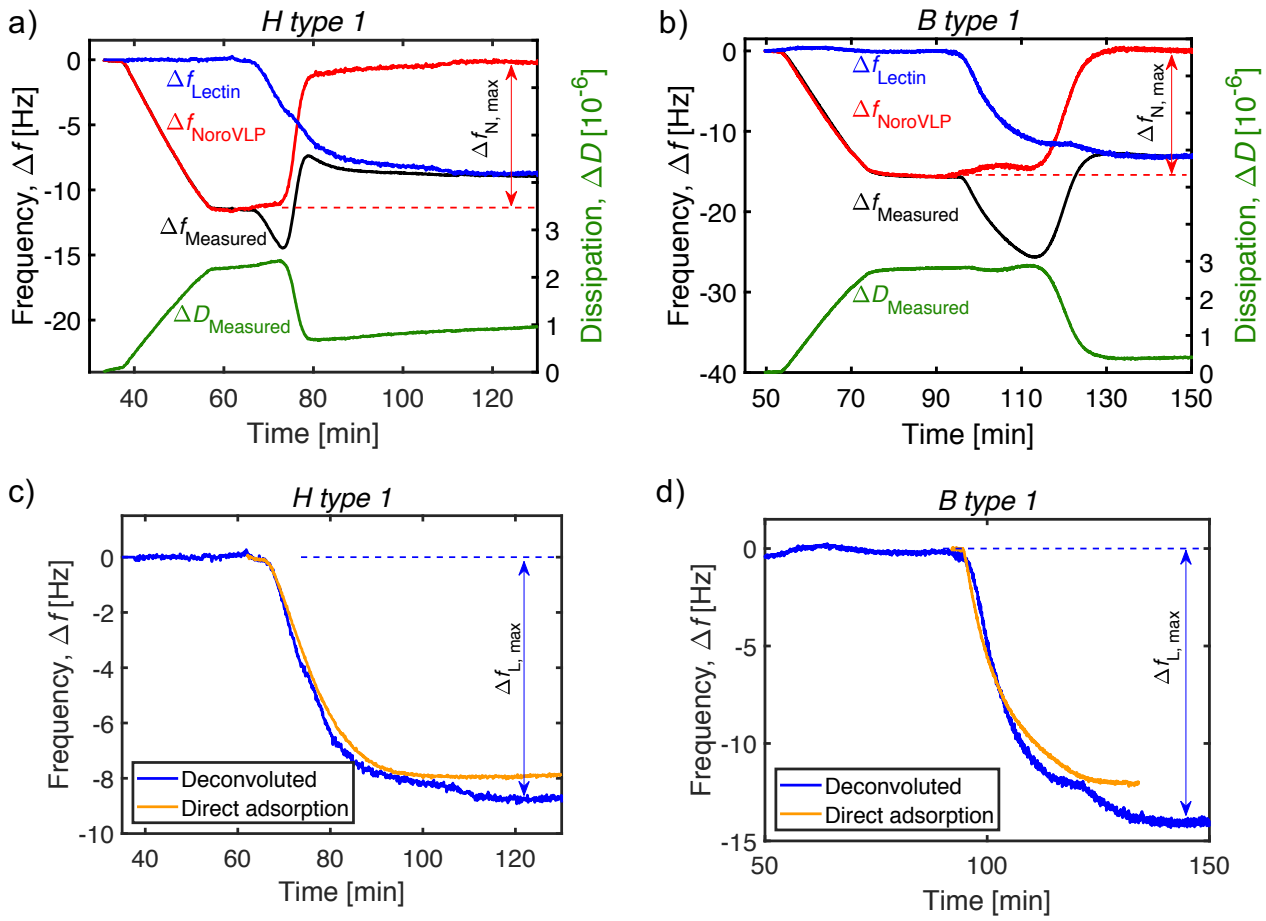

Figure 2. Deconvolution of the measured frequency trace (black line) of noroVLPs bound to a SLB containing (a) 6.3 mol% H type 1 and (b) 3.5 mol% B type 1 at competitive binding. 0.25 nM noroVLP was employed for the virus particle binding. 16 and 160 nM lectin was added to induce competition in case of H and B type 1, respectively. The green line corresponds to the measured dissipation shift, which was used to deconvolute the frequency trace into the contributions causes by noroVLPs (red line) and lectin (blue line), respectively (see Supporting Information for details). (c, d) Comparison of lectin traces that have been extracted from the competition experiments (blue) with those that have been recorded for lectin binding to a bare GSL-containing SLB (*i.e.*, in absence of noroVLPs; orange).

In order to probe if the presence of noroVLPs modifies the attachment kinetics of the lectin, Figures 2c and d compares lectin traces that have been extracted from the competition experiments (blue trace) with those that have been recorded for lectin binding to a bare GSL-containing SLB (*i.e.*,

in absence of noroVLPs; orange trace). Further examples are given in Figure S5 and S7. Inspection of Figures 2c and d suggests that the lectin binds slightly faster to SLBs being incubated with noroVLPs and that the presence of SLB-bound noroVLPs also increases the final lectin surface coverage (indicated by the lower Δf values at saturation; Figure S6). Two plausible explanations of this increased lectin surface coverage are: *i*) the lectins bind with lower valency to the GSLs in the presence of noroVLPs, *e.g.* due to the induction of conformational changes or an increased bilayer tension close to the noroVLPs, thereby allowing more lectins to bind to the same amount of GSLs, and *ii*) noroVLP-binding promotes transfer of GSLs from the lower to the upper leaflet of the SLB. Owing to the large HBGA structure presented by the GSLs, the latter explanation may appear unlikely at first sight, but has in fact already been observed for other multivalent binders (cholera toxin subunit B interacting with the ganglioside GM1)[33]. Interestingly, accounting for an apparent increase in GSL concentration by matching the saturated surface coverage of lectin in both cases (noroVLP–free *versus* noroVLP–engaged SLB), resulted in an almost perfect superposition of the corresponding lectin binding kinetics (Figure S5 and S7), leading to 'effective' total GSL concentration of 6.8 instead of 6.3 mol% H type 1, 3.8 instead of 3.5 mol% B type 1 and so forth.

To compare the noroVLP release kinetics independent of the total GSL concentration used in the experiment, the deconvoluted frequency traces of noroVLP and lectin were normalized with respect to their corresponding maximum surface coverage ($\Delta f_{N,max}$ and $\Delta f_{L,max}$ in Figure 2; see Supporting Table S1 for the determined values). Plotting the normalized surface coverage of noroVLPs, $\Delta f_N(t)/\Delta f_{N,max}$, *versus* the one of the lectin, $\Delta f_L(t)/\Delta f_{L,max}$, allows for assessing the effect of successive GSL depletion (caused by lectin addition) on noroVLP release (Figures 3a and b). The release of noroVLPs follows a sigmoidal curve in dependence of the normalized lectin surface coverage, the inflection point of which shifts to larger $\Delta f_L/\Delta f_{L,max}$ values for an increasing total GSL concentration. This indicates that increasing the total GSL concentration in the SLBs allows more lectins to bind to the SLB before noroVLP release becomes triggered by competition. In order to better understand this effect, we first calculated the fraction of GSLs that are not engaged in lectin

binding. The fraction can be expressed by $1 - \Delta f_L/\Delta f_{L,max}$, as the saturated lectin coverage increases approximately linearly with GSL concentration up to 6.3 mol% H Type 1 and 1.4 mol% B type 1 (deconvoluted lectin coverages in Figure S7). This fraction is expressed with respect of the total GSL concentration embedded in the SLB. Thus, multiplying $1 - \Delta f_L/\Delta f_{L,max}$ by the 'effective' total GSL concentration (discussed above) yields the concentration of GSLs not being bound to a lectin (in units of mol%). Interestingly, upon plotting the noroVLP release versus the total GSL concentration that is not engaged in lectin binding, the corresponding release curves superimpose in case of H type 1 (Figure 3c, circles). In contrast, the noroVLP release curves show minor yet significant deviations for B type 1 (Figure 3d, circles).

In analogy to Figure 1d, the inflection point of these release curves can be used to determine the concentration of GSLs (not being engaged in lectin binding) below which noroVLP release is triggered. This critical GSL concentration for release depends, in contrast to the one of Figure 1d, on various parameters, such as the surface coverage of noroVLPs prior to lectin competition and the minimum number of GSLs that have to be bound to a noroVLP to achieve sufficiently firm attachment on a SLB. Nevertheless, Figure 3c shows two superimposing release curves, which indicates that the critical GSL concentration (3 mol%) of release does not depend on the total GSL concentration in the SLB for H type 1. Furthermore, the critical GSL concentration for H type 1 is only 10% larger than the concentration of the same GSL needed to achieve noroVLP attachment (Figure 3d, solid line *versus* circles; the solid line has been taken from the fit of Figure 1d). Release from B type 1 shows a fundamentally different behavior (Figure 3d, solid line *versus* circles). Here, the critical GSL concentration for release (~0.4 mol%; Figure 3d, circles) is always significantly smaller than the B type 1 concentration needed to achieve noroVLP attachment (Figure 3d, solid line).

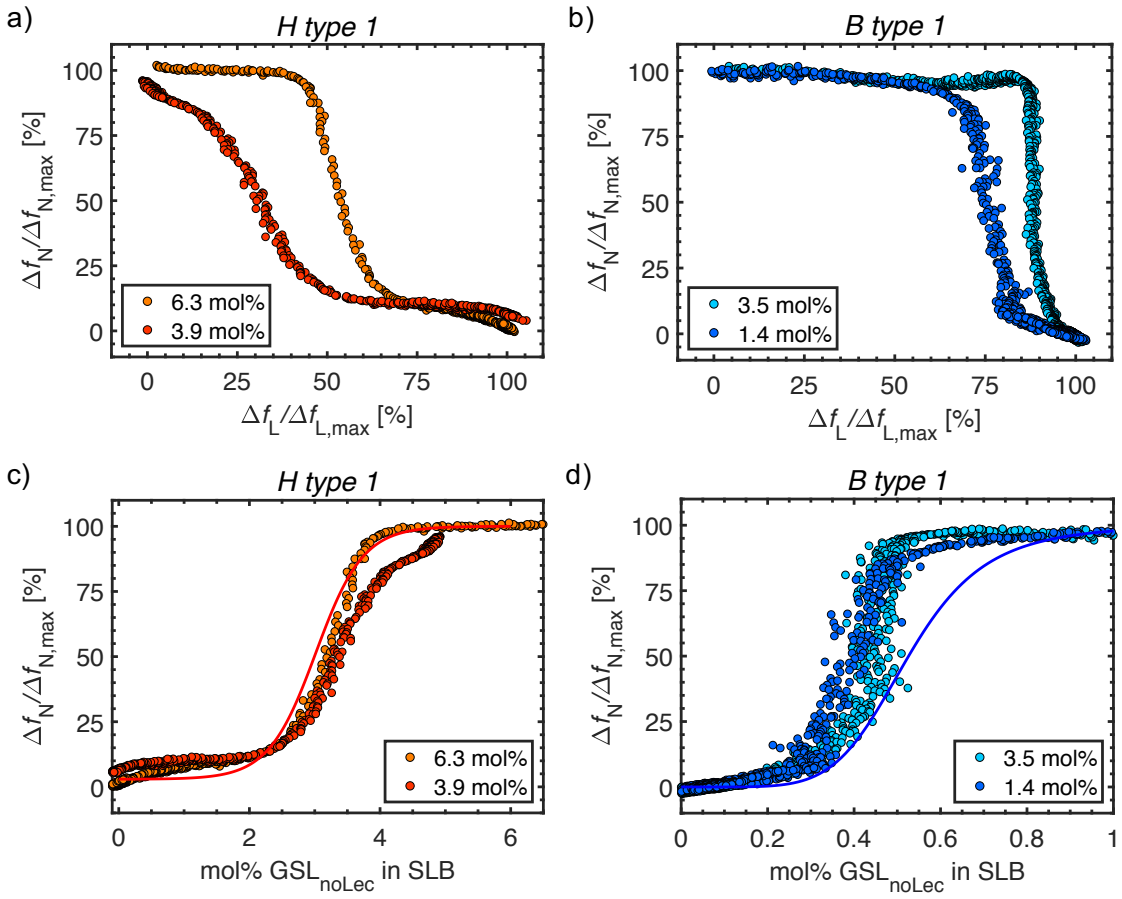

Figure 3. Lectin coverage dependent detachment of SLB-bound noroVLPs. (a, b) A comparison of the relative surface coverages of noroVLPs, $\Delta f_N/\Delta f_{N,max}$, and lectin, $\Delta f_L/\Delta f_{L,max}$, at nominal GSL (H or B type 1) concentrations as indicated. (c, d) The relative noroVLP surface coverage ($\Delta f_N/\Delta f_{N,max}$) *versus* the concentration of GSLs in the SLB that are not engaged in binding to lectins (mol% GSL_{noLec} in SLB; see main text for details). The solid line in Figure 3c and d is a sigmoidal fit of the noroVLP attachment rate vs. GSL concentration in SLB as plotted in Figure 1d.

Discussion and Conclusion

Using a GSL-containing SLB as model lipid membrane, we have explored the attachment of noroVLPs to two different GSLs, H type 1 and B type 1, respectively, and the detachment of SLB-bound noroVLPs caused by addition of a lectin from *Ralstonia solanacearum*. Monitoring the attachment process using QCM-D allowed us to quantify the binding rate of noroVLPs as a function

of GSL type and concentration. The observed binding rate increased with increasing GSL concentration, showing a sigmoidal curve (as often observed when probing multivalent interactions [6, 11, 34-35]) with an inflection point at around 3 mol% H type 1 and 0.5 mol% B type 1. We attribute this large deviation in the inflection points to a much larger affinity of noroVLPs to B type 1 than to H type 1, despite the very small structural difference of these GSLs. Accounting for the fact that the head group area of a single phosphocholine lipid is approximately 0.64 nm^2 (see Ref. 36), GSL concentrations of 0.5 and 3 mol % correspond to densities of 0.008 and 0.047 GSLs per nm^2, respectively. This shows that noroVLPs only bind to H type 1-containing SLBs, if the H type 1 surface density (0.047/nm^2) approaches the density of the HBGA binding pockets on the noroVLP capsid (0.035 or 0.071/nm^2 using the one- or two-binding site model[29-30], respectively). In contrast, binding to B type 1 requires only one-tenth of this density to achieve notable binding rates, which clearly indicates that the noroVLP interaction with H type 1 GSLs is much weaker than that to B type 1.

We also quantified the release of GSL-bound noroVLPs by addition of a lectin, and used a deconvolution method to separate the detachment kinetics of noroVLPs from the lectin attachment kinetics from the measured QCM-D traces for both GSL types and at various GSL concentrations. As the lectin has different binding kinetics (affinity) towards the two GSLs, which may influence the observed differences in the noroVLP release kinetics, a direct comparison of the correspondingly measured and deconvoluted release kinetics was not straightforward. To address this challenge, we used the lectin surface coverage to calculate (during competition) the concentration of GSLs that are not engaged in lectin binding, GSL_{noLec}, and correlated the noroVLP surface coverage with GSL_{noLec} (Figures 3c and d). Similar to Figure 1d, the noroVLP surface coverage exhibits a sigmoidal dependence on GSL_{noLec} and showed that release of noroVLPs is induced at low GSL_{noLec} values. Interestingly, the traces of the H type 1 measurements overlap very well in this plot, despite the appreciable difference in total GSL concentration used. Furthermore, the inflection point of these traces, *i.e.*, the GSL_{noLec} concentration below which release of noroVLPs is induced, is only 10% larger than the corresponding inflection point in Figure 1d. This shift can be attributed to the fact that

the abscissa, GSL_{noLec}, in Figure 3c represents the concentration of GSLs not being engaged in any binding ("free GSLs") plus the concentration of noroVLP-bound GSLs, while in Figure 1d only the concentration of free GSLs is shown (as the initial binding rate was determined at the beginning of the binding process, *i.e.*, at negligible noroVLP surface coverage). Hence, even under GSL-VLP attachment equilibrium conditions, the release curves of Figure 3c are expected to be shifted to higher concentrations with respect to the binding rate curves of Figure 1d, which expresses the minimum GSL concentration required for a firm attachment of noroVLPs on SLB.

Interestingly, noroVLP release from B type 1 showed a fundamentally different behaviour, as all release curves yielded inflection points at lower concentrations with respect to the corresponding binding rate curve of Figure 1d, a feature that cannot be explained by differences in noroVLP surface coverage (see Figure 1c). Additionally, as GSL_{noLec} represents the sum of free and noroVLP-engaged GSLs, the actual concentration of free B type 1 GSLs in the SLB is even lower than indicated by the x-axis of Figure 3d. This means that release of noroVLPs from B type 1 occurs at free B type 1 concentrations that are far below the concentration needed to achieve initial noroVLP attachment to the SLB (Figure 1d). In other words, once bound to a B type 1-containing SLB, the noroVLPs are able to remain firmly attached to the SLB even at GSL concentrations at which they would not be able to initiate firm attachment from solution. This clearly indicates that the noroVLPs accumulate B type 1 GSLs in the interaction area with the SLB, *i.e.*, the total GSL concentration (free plus noroVLP-engaged) is larger in the noroVLP-SLB interaction area than in SLB areas not being engaged in noroVLP interactions. Such an accumulation cannot be ruled out for the interaction with H type 1 GSLs, but it has to be much smaller in comparison to B type 1 GSLs. This is consistent with their large difference in affinity towards noroVLPs, since a higher affinity of the noroVLP towards B type 1 may favour accumulation of GSLs underneath the SLB-bound viruses.

Irrespective of some variance in the inflection point of the B type 1 release curve, it is evident from Figure 3c and d that release of noroVLPs occurs at much lower GSL_{noLec} values for B type 1

compared with H type 1. In analogy to the binding rate curves, this again indicates that noroVLPs have a higher affinity towards B type 1 than to H type 1. This finding is supported by the energy of single noroVLP-GSL bond determined from the competitive release kinetics at 6.3 mol% H type 1 and 3.5 mol% B type 1, respectively, at which the noroVLP surface coverage is far from saturation. The corresponding estimates were done analytically as earlier described in detail in the case of the interaction of SV40 with the lipid GM1.[6] As input, we need the maximum number of the ligand-receptor bonds in the contact zone, the release time scale, and the scale of the fraction (or concentration) of unbound GSL (with respect to the total number of lipids in SLB) during the release. Calculating with 360 binding sites per VLP, the maximum number of bonds, $n \cong 12$, was obtained by taking the norovirus geometry (or, more specifically, the virus radius and the area of the binding sites) into account as it was earlier done for noro- and SV40 viruses.[4,6] The release time scale, $\tau = 5$ and 10 min (in the cases of H type 1 and B type 1, respectively), was estimated from the kinetics measured (Figure 2a and b). The fraction of unbound GSL, $\theta_{un} = 0.03$ and 0.004 (H type 1 and B type 1), was estimated on the basis of the release (or attachment) kinetics (e.g., Figure 3c and d). With this input, we obtained (see Section "Estimation of the GSL-noroVLP binding energies" in the Supporting Information) that the single noroVLP-H type 1 and B type 1 bond energies are ~ 3.5 and 4.5 kcal/mol, respectively. The sensitivity of the estimates of this energy to the input parameters, τ and θ_{un}, is logarithmically weak. For this reason, the difference in the energies is small. Calculating with 180 binding sites, which is a relevant comparison,[37] instead yields a maximum number of bonds of $n \cong 6$, leading to bond energies of ~ 5 and 6 kcal/mol, respectively.

The extracted binding energies are very similar (360 binding site model) to, and a factor of 2 larger (180 binding site model) than, the values reported in a recent study,[37] in which K_d values for the interaction of noroVLP P-dimers with methyl α-l-fucopyranoside or the blood group B trisaccharide α-l-Fuc-(1,2)-[α-d-Gal-(1,3)-]-α-d-Gal-(1,N)-N_3 have been determined using NMR. The good agreement with literature values could be taken as indication that the 360 binding site model is more

likely to represent the binding mode of noroVLPs towards GSLs. We cannot exclude, however, that deviations in the extracted binding energies can be attributed to the fact that different carbohydrates were used in the NMR and QCM-D experiments: While (water soluble) methyl α-l-fucopyranoside and a blood group B trisaccharide were used in the NMR study, complete GSLs were used in our QCM-D study, presenting either a penta- (H type 1) or hexasaccharide (B type 1), respectively. Hence, minor differences in the binding energies are here not sufficient to generally rule out the appropriateness of the 180 binding site model, as these differences may simply reflect differences in the structure of the used carbohydrates. In fact, molecular dynamics simulations with the VA387 GII.4 B-trisaccharide co-crystal structure have suggested that the binding strength is increased when the trisaccharide is extanded to the B type 1 tetrasaccharide.[38]

Furthermore, the above-mentioned NMR study[37] also shows that the unusual binding behaviour of noroVLPs to HBGAs, which has led to the identification of the second fucose binding site of VP1, can be related to a spontaneous deamidation of an asparagine residue in the HBGA binding pocket. This study therefore suggests that the second fucose binding site is only of minor importance in HBGA binding of the GII.4 strain and makes the 180 binding site model more realistic.[37] We therefore decided to provide the binding energies extracted using both models, as the 360 binding site model is in better agreement with reported values, while the 180 binding site model is better supported by recent biochemical characterizations of the VP1-HBGA interaction.[37]

It is important to note that the HBGA binding pocket lowers its ability to bind HBGAs upon spontaneous deamidation of the asparagine residue, a process that has a half-time of 1.5 days at 37°C.[37] Although we cannot rule out the occurrence of spontaneous deamidation during the production of our noroVLPs, a process which would reduce the effective number of binding sites below 180 or 360 per noroVLP, respectively, we can rule out any significant impact of deamidation during noroVLP storage (at 4°C) or the biophysical characterization using QCM-D (at room temperature). This follows from the observation that we did not observe significant changes between

identical QCM-D measurements performed within a period of 3 months and as the timescale of a QCM-D experiment is on the order of few hours (in contrast to the half-time of 1.5 days reported for the spontaneous deamidation). Hence, the reported binding energies should be understood as lower limits, as deamidation cannot be fully ruled out and would reduce the number of available binding sites per noroVLP.

Compared to our previous study of the competition for GSLs between SV40 and recombinant cholera toxin B subunit, in which we quantified the bond energy of SV40-GSL from the virus release kinetics,[6] the data of the present study demonstrate in addition that the noroVLP binding affinity/strength towards different GSLs can be compared by analyzing either their binding kinetics to a GSL-containing SLB or their release kinetics from the lectin-induced by competition. In the former case, the GSL concentration at the transition from reaction- to diffusion-limited binding kinetics of noroVLP reflects the binding strength of noroVLPs to the different GSLs: A decrease in transition concentration indicates an increase in the binding strength of the noroVLP towards the particular GSL. However, experiments using multiple SLBs with different GSL concentrations is required to obtain such transition curves, which may in addition suffer from uncertainties, particularly, with respect to handling low GSL concentrations such as in case of B type 1. In contrast, in the competition approach a *single* kinetic measurement per GSL type is sufficient to qualitatively compare the binding strength of noroVLPs towards different GSLs, provided that the noroVLP coverage before injecting the lectin is above the detection limit and similar in the corresponding measurements (see Figure 1). The general relevance of this approach is obvious from the fact that conceptually identical analysis can be done for a range of norovirus attachment factors with a difference in the binding affinity even lower than that of B and H type 1, and also for any virus for which competitive binding can be experimentally realized. This typically only requires the existence of a second species (*e.g.*, a lectin in the current case), which possesses binding sites with higher binding affinity to the receptors/attachment factors than the ones of the virion/VLP; an exact knowledge of the involved affinities is not required.

In addition to an intrinsic interest, the competitive binding under consideration is also useful in the context of quantification the strength of the ligand-receptor bonds responsible for the interaction of viruses with lipid membranes or, more specifically, in the context of the development of inhibitors targeting either viruses[12, 39-40] or their receptors/virus attachment factors.[15-16, 41] These inhibitors aim to block the virus attachment on cell membranes and to do so they need a sufficiently high affinity/binding strength towards the target. Unlike monovalent ligand-receptor interactions, virus-receptor interactions on cell-membranes are typically multivalent. Under this condition, thermodynamic methods such as ITC can provide the binding affinity/energy of a single virus-receptor bond, but they are unable to evaluate the absolute binding strength of viruses being attached to the membrane-embedded ligands. In this regard, surface-based kinetic assays better represent the native plasma membrane environment. In these assays, the ratio of association (k_{on}) and dissociation (k_{off}) rate constant upon virus binding to receptors tethered to the surface or embedded in lipid-membrane represents the dissociation constant (K_d) of the virus-receptor pair, a measure of the binding affinity. Although single virus-receptor bonds are assumed to form and dissociate continuously, the cumulative effect from the multivalent interaction makes the virus attachment to appear irreversible. This hinders determination of k_{off} and thereby K_d. Diminishing the multivalent interaction by lowering the receptor density leads to a transient binding with weak association rate, which becomes difficult to quantify with standard experimental techniques. In contrast, the competition approach used here may still be operative to probe both attachment and detachment kinetics of viruses on membranes and thereby, for the determination of their relative binding affinity/energy.

Finally it is worth emphasizing that at native conditions, the receptor/attachment factor concentration in the plasma membrane influences the absolute binding strength of viruses, as indicated by *in vivo* studies of infection susceptibility of other caliciviruses.[42] At cellular infection, the virus coverage on the plasma membrane is likely to be far from saturation and membrane receptors are typically in excess. These conditions are suitable for both comparative and quantitative analysis

of competition kinetics. Hence, our approach to scrutinize multivalent virus-receptor interactions might be applicable also beyond the model systems used in this work. This aspect is obviously particularly useful in screening for new receptors of emerging strains of highly mutating viruses, such as human norovirus, as well as for the development of antiviral drugs.

ACKNOWLEDGEMENTS

This work was supported by the Swedish research council (grant numbers 2017-00955, 2018-04900), the German Research Foundation (grant number BL1514/1), and the Academy of Finland (grant no. 290506). We acknowledge Biocenter Finland for infrastructure support.

ASSOCIATED CONTENT

Supporting Information. The Supplementary Information contains supporting data from QCM-D and SPR experiments. Furthermore, 2 Supporting Movies are provided, showing the release of noroVLPs from a H type 1- and B type 1-containing SLB upon lectin addition. This material is available free of charge via the Internet at xxx.

AUTHOR INFORMATION

Corresponding Authors

* Email: nagma.parveen@kuleuven.be (N.P.), fredrik.hook@chalmers.se (F.H.), stephan.block@fu-berlin.de (S.B.).

ORCIDs

Nagma Parveen: 0000-0003-4577-7721

Göran Larson: 0000-0002-2616-0366

Vesa P. Hytönen: 0000-0002-9357-1480

Vladimir P. Zhdanov: 0000-0002-0167-8783

Fredrik Höök: 0000-0003-1994-5015

Stephan Block: 0000-0002-2947-0837

NOTES

The authors have no competing financial interests.

References

1. Boulant, S.; Stanifer, M.; Lozach, P.-Y., Dynamics of virus-receptor interactions in virus binding, signaling, and endocytosis. *Viruses* **2015,** *7* (6), 2794-2815.
2. Di Michele, L.; Jana, P. K.; Mognetti, B. M., Steric interactions between mobile ligands facilitate complete wrapping in passive endocytosis. *Phys. Rev. E* **2018,** *98* (3), 032406.
3. Parveen, N.; Borrenberghs, D.; Rocha, S.; Hendrix, J., Single Viruses on the Fluorescence Microscope: Imaging Molecular Mobility, Interactions and Structure Sheds New Light on Viral Replication. *Viruses* **2018,** *10* (5), 250.
4. Bally, M.; Gunnarsson, A.; Svensson, L.; Larson, G.; Zhdanov, V. P.; Hook, F., Interaction of single viruslike particles with vesicles containing glycosphingolipids. *Phys. Rev. Lett.* **2011,** *107* (18), 188103.
5. Neu, U.; Woellner, K.; Gauglitz, G.; Stehle, T., Structural basis of GM1 ganglioside recognition by simian virus 40. *Proc. Natl. Acad. Sci. U.S.A.* **2008,** *105* (13), 5219-5224.
6. Parveen, N.; Block, S.; Zhdanov, V. P.; Rydel, G. E.; Hook, F., Detachment of membrane bound virions by competitive ligand binding induced receptor depletion. *Langmuir* **2017,** *33* (16), 4049-4056.
7. Nasir, W.; Bally, M.; Zhdanov, V. P.; Larson, G.; Höök, F., Interaction of Virus-Like Particles with Vesicles Containing Glycolipids: Kinetics of Detachment. *J. Phys. Chem. B* **2015,** *119* (35), 11466-11472.
8. Fasting, C.; Schalley, C. A.; Weber, M.; Seitz, O.; Hecht, S.; Koksch, B.; Dernedde, J.; Graf, C.; Knapp, E.-W.; Haag, R., Multivalency as a Chemical Organization and Action Principle. *Angew. Chem. Int. Ed.* **2012,** *51* (42), 10472-10498.
9. Mammen, M.; Choi, S. K.; Whitesides, G. M., Polyvalent interactions in biological systems: Implications for design and use of multivalent ligands and inhibitors. *Angew. Chem. Int. Ed.* **1998,** *37* (20), 2755-2794.
10. Rydell, G. E.; Dahlin, A. B.; Hook, F.; Larson, G., QCM-D studies of human norovirus VLPs binding to glycosphingolipids in supported lipid bilayers reveal strain-specific characteristics. *Glycobiology* **2009,** *19* (11), 1176-1184.
11. Szklarczyk, O. M.; Gonzalez-Segredo, N.; Kukura, P.; Oppenheim, A.; Choquet, D.; Sandoghdar, V.; Helenius, A.; Sbalzarini, I. F.; Ewers, H., Receptor concentration and diffusivity control multivalent binding of SV40 to membrane bilayers. *PLoS Comput. Biol.* **2013,** *9* (11), e1003310.
12. Mammen, M.; Dahmann, G.; Whitesides, G. M., Effective inhibitors of hemagglutination by influenza-virus synthesized from polymers having active ester groups - insight into mechanism of inhibition. *J. Med. Chem.* **1995,** *38* (21), 4179-4190.
13. Patching, S. G., Surface plasmon resonance spectroscopy for characterisation of membrane protein–ligand interactions and its potential for drug discovery. *Biochimica et Biophysica Acta (BBA) - Biomembranes* **2014,** *1838* (1, Part A), 43-55.
14. Tabarani, G.; Reina, J. J.; Ebel, C.; Vivès, C.; Lortat-Jacob, H.; Rojo, J.; Fieschi, F., Mannose hyperbranched dendritic polymers interact with clustered organization of DC-SIGN and inhibit gp120 binding. *FEBS Lett.* **2006,** *580* (10), 2402-2408.
15. Chen, Q.; Guo, Y., Influenza viral hemagglutinin peptide inhibits influenza viral entry by shielding the host receptor. *ACS Infect. Dis.s* **2016,** *2* (3), 187-193.
16. Dragic, T.; Trkola, A.; Thompson, D. A. D.; Cormier, E. G.; Kajumo, F. A.; Maxwell, E.; Lin, S. W.; Ying, W. W.; Smith, S. O.; Sakmar, T. P.; Moore, J. P., A binding pocket for a small molecule

inhibitor of HIV-1 entry within the transmembrane helices of CCR5. *Proc. Natl. Acad. Sci. U.S.A.* **2000,** *97* (10), 5639-5644.
17. Porotto, M.; Yokoyama, C. C.; Palermo, L. M.; Mungall, B.; Aljofan, M.; Cortese, R.; Pessi, A.; Moscona, A., Viral entry inhibitors targeted to the membrane site of action. *J. Virol.* **2010,** *84* (13), 6760-6768.
18. De Clercq, E.; Li, G., Approved Antiviral Drugs over the Past 50 Years. *Clin. Microbiol. Rev.* **2016,** *29* (3), 695.
19. Fang, F.; Szleifer, I., Competitive adsorption in model charged protein mixtures: equilibrium isotherms and kinetics behavior. *J. Chem. Phys* **2003,** *119* (2), 1053-1065.
20. Kimura-Suda, H.; Petrovykh, D. Y.; Tarlov, M. J.; Whitman, L. J., Base-Dependent Competitive Adsorption of Single-Stranded DNA on Gold. *J. Am. Chem. Soc.* **2003,** *125* (30), 9014-9015.
21. Jana, P. K.; Mognetti, B. M., Surface-triggered cascade reactions between DNA linkers direct the self-assembly of colloidal crystals of controllable thickness. *Nanoscale* **2019,** *11* (12), 5450-5459.
22. Hutson, A. M.; Atmar, R. L.; Marcus, D. M.; Estes, M. K., Norwalk virus-like particle hemagglutination by binding to H histo-blood group antigens. *J. Virol.* **2003,** *77* (1), 405-415.
23. Lindesmith, L. C.; Donaldson, E. F.; Lobue, A. D.; Cannon, J. L.; Zheng, D. P.; Vinje, J.; Baric, R. S., Mechanisms of GII.4 norovirus persistence in human populations. *PLos Med.* **2008,** *5* (2), 269-290.
24. Kostlánová, N.; Mitchell, E. P.; Lortat-Jacob, H.; Oscarson, S.; Lahmann, M.; Gilboa-Garber, N.; Chambat, G.; Wimmerová, M.; Imberty, A., The Fucose-binding Lectin from Ralstonia solanacearum: a new type of β-propeller architecture formed by oligomerization and interacting with fucoside, fucosyllactose, and plant xyloglucan. *J. Biol. Chem.* **2005,** *280* (30), 27839-27849.
25. Rydell, G. E.; Svensson, L.; Larson, G.; Johannes, L.; Romer, W., Human GII.4 norovirus VLP induces membrane invaginations on giant unilamellar vesicles containing secretor gene dependent alpha 1,2-fucosylated glycosphingolipids. *Biochim. Biophys. Acta-Biomembr.* **2013,** *1828* (8), 1840-1845.
26. Nilsson, J.; Rydell, G. E.; Le Pendu, J.; Larson, G., Norwalk virus-like particles bind specifically to A, H and difucosylated Lewis but not to B histo-blood group active glycosphingolipids. *Glycoconjugate J.* **2009,** *26* (9), 1171-1180.
27. Karlsson, K. A.; Larson, G., Molecular characterization of cell-surface antigens of fetal tissue - detailed analysis of glycosphingolipids of meconium of a human-o le(a-b+) secretor. *J. Biol. Chem.* **1981,** *256* (7), 3512-3524.
28. Koho, T.; Ihalainen, T. O.; Stark, M.; Uusi-Kerttula, H.; Wieneke, R.; Rahikainen, R.; Blazevic, V.; Marjomaki, V.; Tampe, R.; Kulomaa, M. S.; Hytonen, V. P., His-tagged norovirus-like particles: A versatile platform for cellular delivery and surface display. *Eur. J. Pharm. Biopharm.* **2015,** *96*, 22-31.
29. Cao, S.; Lou, Z.; Tan, M.; Chen, Y.; Liu, Y.; Zhang, Z.; Zhang, X. C.; Jiang, X.; Li, X.; Rao, Z., Structural Basis for the Recognition of Blood Group Trisaccharides by Norovirus. *J. Virol.* **2007,** *81* (11), 5949.
30. Mallagaray, A.; Lockhauserbäumer, J.; Hansman, G.; Uetrecht, C.; Peters, T., Attachment of Norovirus to Histo Blood Group Antigens: A Cooperative Multistep Process. *Angew. Chem. Int. Ed* **2015,** *54* (41), 12014-12019.
31. Cho, N.-J.; Frank, C. W.; Kasemo, B.; Höök, F., Quartz crystal microbalance with dissipation monitoring of supported lipid bilayers on various substrates. *Nat. Protoc.* **2010,** *5*, 1096.
32. Parveen, N.; Rimkute, I.; Block, S.; Rydell, G. E.; Midtvedt, D.; Larson, G.; Hytonen, V. P.; Zhdanov, V. P.; Lundgren, A.; Hook, F., Membrane Deformation Induces Clustering of Norovirus Bound to Glycosphingolipids in a Supported Cell-Membrane Mimic. *J. Phys. Chem. Lett.* **2018,** *9* (9), 2278-2284.
33. Carton, I.; Malinina, L.; Richter, R. P., Dynamic Modulation of the Glycosphingolipid Content in Supported Lipid Bilayers by Glycolipid Transfer Protein. *Biophys. J.* **2010,** *99* (9), 2947-2956.

34. Müller, M.; Lauster, D.; Wildenauer, H. H. K.; Herrmann, A.; Block, S., Mobility-Based Quantification of Multivalent Virus-Receptor Interactions: New Insights Into Influenza A Virus Binding Mode. *Nano Letters* **2019,***19* (3), 1875-1882.
35. Xu, H.; Shaw, D. E., A Simple Model of Multivalent Adhesion and Its Application to Influenza Infection. *Biophys. J.* **2016,** *110* (1), 218-233.
36. König, B.; Dietrich, U.; Klose, G., Hydration and Structural Properties of Mixed Lipid/Surfactant Model Membranes. *Langmuir* **1997,** *13* (3), 525-532.
37. Mallagaray, A.; Creutznacher, R.; Dulfer, J.; Mayer, P. H. O.; Grimm, L. L.; Orduna, J. M.; Trabjerg, E.; Stehle, T.; Rand, K. D.; Blaum, B. S.; Uetrecht, C.; Peters, T., A post-translational modification of human Norovirus capsid protein attenuates glycan binding. *Nat. Commun.* **2019,** *10*, 14.
38. Koppisetty, C. A.; Nasir, W.; Strino, F.; Rydell, G. E.; Larson, G.; Nyholm, P.-G., Computational studies on the interaction of ABO-active saccharides with the norovirus VA387 capsid protein can explain experimental binding data. *Journal of computer-aided molecular design* **2010,** *24* (5), 423-431.
39. Bovin, N. V.; Tuzikov, A. B.; Chinarev, A. A.; Gambaryan, A. S., Multimeric glycotherapeutics: New paradigm. *Glycoconjugate J.* **2004,** *21* (8-9), 471-478.
40. Waldmann, M.; Jirmann, R.; Hoelscher, K.; Wienke, M.; Niemeyer, F. C.; Rehders, D.; Meyer, B., A nanomolar multivalent ligand as entry inhibitor of the hemagglutinin of avian influenza. *J. Am. Chem. Soc.* **2014,** *136* (2), 783-788.
41. Dorr, P.; Westby, M.; Dobbs, S.; Griffin, P.; Irvine, B.; Macartney, M.; Mori, J.; Rickett, G.; Smith-Burchnell, C.; Napier, C.; Webster, R.; Armour, D.; Price, D.; Stammen, B.; Wood, A.; Perros, M., Maraviroc (UK-427,857), a potent, orally bioavailable, and selective small-molecule inhibitor of chemokine receptor CCR5 with broad-spectrum anti-human immunodeficiency virus type 1 activity. *Antimicrobial Agents and Chemotherapy* **2005,** *49* (11), 4721-4732.
42. Ruvoën-Clouet, N.; Ganière, J. P.; André-Fontaine, G.; Blanchard, D.; Le Pendu, J., Binding of rabbit hemorrhagic disease virus to antigens of the ABH histo-blood group family. *J. Virol.* **2000,** *74* (24), 11950-11954.

Table of content